Astron. Astrophys. 335, 123–133 (1998)

ASTRONOMY AND ASTROPHYSICS

Spiral pattern in the optical polarization of NGC 6946

Ch. Fendt[1,2,⋆], **R. Beck**[3], **and N. Neininger**[4]

[1] Astrophysikalisches Institut Potsdam, An der Sternwarte 16, D-14482 Potsdam, Germany (cfendt@aip.de)
[2] Landessternwarte Königstuhl, D-69117 Heidelberg, Germany
[3] Max-Planck-Institut für Radioastronomie, Auf dem Hügel 69, D-53121 Bonn, Germany (rbeck@mpifr-bonn.mpg.de)
[4] Radioastronomisches Institut der Universität Bonn, Auf dem Hügel 71, D-53121 Bonn, Germany (nneini@astro.uni-bonn.de)

Received 26 February 1998 / Accepted 16 March 1998

Abstract. Wide-field images of NGC 6946 in linear optical polarization are presented. In large parts of the galaxy the polarization pattern delineates a spiral structure, in partial agreement with the radio polarization data. A possible explanation of such a pattern is the alignment of elongated dust grains in the regular interstellar magnetic field.

The optical degree of polarization anti-correlates with the stellar density: the bright parts of the spiral arms and the nuclear region reveal the lowest degrees of polarization (below 0.5%), while the outer, less active regions are significantly polarized (up to 5%). This trend is similar as in the degree of polarization of radio synchrotron emission. This behavior could be interpreted as field tangling in star-forming regions. The higher resolution of our optical data would then allow to determine a new upper limit of the turbulence scale of $\simeq 120$ pc.

In the southern and southwestern parts of NGC 6946 the polarization angles deviate from a spiral structure, indicating the exceptional character of these regions as known from observations in other frequency bands. However, we cannot exclude that here the optical polarization structure is influenced by effects external to the galaxy. The southern region of strong optical polarization and constant vector orientation might be interpreted as enhanced foreground polarization in a Galactic gas/dust cloud.

Key words: polarization – galaxies: individual: M 82 – galaxies: individual: NGC 6946 – galaxies: ISM – galaxies: magnetic fields

1. Optical polarimetry of galaxies

It is well known that light from stars (Hiltner 1949; Hall 1949) and galaxies (Elvius 1951; 1956) may be linearly polarized. Linear optical polarization arises from two "competing" physical processes: (i) anisotropic scattering (AS) by spherical particles (dust and/or gas), and (ii) selective extinction by elongated dust grains aligned by a large-scale magnetic field, where the alignment has become known as Davis-Greenstein mechanism (DGM; Davis & Greenstein 1951, Spitzer 1978).

The interpretation of optical polarization therefore depends on the distributions of light, dust grains and magnetic field, all of which are expected to vary strongly from object to object and also within different parts of the object. Unfortunately, the DGM works only for stars behind a layer of scatterer, i.e. dust clouds or dusty disks in galaxies, which inevitably produce strong extinction and thus lower the signal and increase the errors.

Scattered light is polarized perpendicular to the scattering plane, which is defined by the propagation vectors of the incoming and outgoing light ray, while for DGM the polarization vector is parallel to the magnetic field. A spiral polarization pattern in face-on galaxies might be interpreted as caused by the DGM in the interstellar magnetic field (e.g. M 51, Scarrott et al. 1987; NGC 1068, Scarrott et al. 1991a), because a regular field is of spiral shape according to radio synchrotron observations (Beck et al. 1996).

A circular pattern, as observed e.g. around M 82 (Bingham et al. 1976; Scarrott et al. 1991b), is a clear indication for AS, especially if a bright galactic nucleus is also the scattering source (NGC 7331; Elvius 1956; King 1986). Light from a point-like central source and scattered in an optically thin medium cannot generate a spiral pattern. The scattering properties of a spiral arm environment might possibly produce a spiral pattern, but no modeling has yet been attempted.

In edge-on galaxies with toroidal (plane-parallel) magnetic field the optical polarization from AS and DGM is believed to be perpendicular to each other. However, the situation becomes less clear if also a poloidal (vertical) field are taken into account. While for NGC 891 Scarrott & Draper (1996) [1] found "evidence for vertical magnetic field", Fendt et al. (1996) came to the conclusion that the optical polarization is most probably caused by AS.

Scattering model calculations show that in edge-on galaxies extinction leads to a polarization pattern perpendicular to the major axis and to a circular pattern in face-on galaxies (Bianchi et al. 1996). Depending on the bulge luminosity in terms of

Send offprint requests to: Christian Fendt, Potsdam

⋆ Part of this work was carried out during a visit of C.F. at the MPIfR in Bonn

[1] However, these authors misinterpreted the radio polarization vectors in NGC 891: The field orientation is mainly parallel, *not* vertical to the galaxy's plane.

the total luminosity the circular pattern for inclined galaxies becomes asymmetric in fractional polarization (but not in polarization angle).

Recent modeling of infrared polarimetry (Wood & Jones 1997, Wood 1997) indicates that in edge-on galaxies an undisturbed disk is necessary to clearly distinguish between the two explanations. They succeeded in modeling the calm disk of NGC 4565, but failed for the more disturbed NGC 891. In face-on galaxies the two patterns of AS and DGM become virtually indistinguishable (Wood 1997). However, the model includes a purely toroidal magnetic field, i.e. no spiral magnetic field as observed for NGC 6946.

In this paper, we present linear optical polarization observations of the face-on spiral galaxy NGC 6946. For a more detailed discussion of the instrument, the data reduction, and the error treatment we refer to Fendt et al. 1996 (hereafter P1).

2. The face-on spiral galaxy NGC 6946

NGC 6946 is a Scd galaxy located at $\alpha(1950) = 20^h33^m48\overset{s}{.}8$, $\delta(1950) = 59°58'50''$. It is therefore located at a low galactic latitude of $11\overset{\circ}{.}7$. The inclination is about $\simeq 30°$ (Rogstad & Shostak 1973), or $42°$ (Tully 1988). With our instrument and data reduction we resolve $\simeq 1\overset{''}{.}5$ corresponding to 40 pc, if we assume a distance of 5.5 Mpc (Tully 1988; distance estimates given in the literature vary from 5 Mpc to 11 Mpc).

NGC 6946 exhibits a complicated spiral structure. Six optical arms emanate from the center (Tacconi & Young 1990). The three arms originating north-east oft the center are well developed, while the structure of the other arms in the south-western quadrant is poorly defined. With the method of wavelet analysis applied on a red-light image, Frick et al. (1998) detected a dominating two-armed spiral pattern in the inner galaxy (below 6 kpc radius) and a three-armed pattern at larger radii.

Thanks to its large angular extent on sky and lack of any companion galaxy, NGC 6946 became one of the prototype spiral galaxies and was extensively studied in all frequency bands.

RADIO. NGC 6946 is a strong source in radio continuum with highest intensities on the spiral arms (Klein et al. 1982; Beck & Hoernes 1996). Linearly polarized synchrotron emission revealed an overall magnetic field with a spiral pattern (Klein et al. 1982; Harnett et al. 1989; Beck 1991; Ehle & Beck 1993). Recent observations with high angular resolution showed that the strongest regular magnetic fields do not coincide with the optical arms, but are located in interarm regions, forming two major "magnetic arms" (Beck & Hoernes 1996). The phase shift in azimuthal angle between the magnetic arms and the optical arms preceding in the sense of galactic rotation is almost constant at all galactic radii (Frick et al. 1998). Within the optical spiral arms the degree of radio polarization is very low, in spite of the relatively high total radio intensity. This tells us that the magnetic field in the optical spiral arms must be tangled on scales smaller than the telescope resolution ($\simeq 330$ pc at the assumed distance to NGC 6946).

Tacconi & Young (1986; 1989; 1990), Carignan et al. (1990) and Kamphuis & Sancisi (1993) observed NGC 6946 in the HI and CO radio lines. The total extent in HI is more than 30 kpc, about twice the radius in optical and radio continuum emission. Ishizuki et al. (1990) found a molecular CO bar extending 1.7 kpc from the galaxy center with P.A. 140°. CO together with K-band images showed evidence for four spiral arms, which is, however, not a common property of barred spiral galaxies (Regan & Vogel 1995).

INFRARED. Warm dust is observed in FIR continuum maps (Smith et al. 1984; Engargiola & Harper 1992). Observations with the *Kuiper Airborne Observatory* of the 158μm [CII] fine-structure line (Madden et al. 1993) showed emission from three spatially distinct components – nucleus, spiral arms and an extended disk of 12 kpc radius. NGC 6946 was one of the main targets for the *ISO* satellite. The observations covered the rotational H_2 lines (Valentijn et al. 1996), FIR continuum maps (Tuffs et al. 1996; Lu et al. 1996), and mid-IR maps (Helou et al. 1996; Malhotra et al. 1996).

OPTICAL LINES. Roy & Belley (1993) obtained narrow-band images in Hα, Hβ, [OIII], and [NII] in order to compare them with the molecular CO. They concluded that the inner molecular bar is associated with enhanced massive star formation. A map of the large-scale Hα emission was given by Ehle & Beck (1993).

X-RAY. *ROSAT* observations (Schlegel 1994) revealed diffuse extended emission of a very hot component of the galaxy's ISM and resolved three nuclear (point) sources and also the bright northern spiral arm.

3. Instrument, observations and data reduction

The observations were performed at the 1.23 m telescope of the DSAZ[2] (Deutsch-Spanisches Astronomisches Zentrum), Calar Alto, Spain, using the CCD polarimeter of the Landessternwarte Heidelberg, Germany. The total exposure time was 16x15 min, giving redundant samples of the polarization orientation. Cataloged polarized standard stars were used for calibration. The seeing was about $3''$. During the observation of NGC 6946 it was almost new moon. The lunar position (at 23.00 UT: $\alpha = 10^h35^m$, $\delta = 6°55'$) was such, that the polarization angle of scattered moon light would be at P.A.$\simeq 90°$.

The instrument consists of a focal reducer (reduction factor 3.43; field of view $14\overset{'}{.}4$ x $9\overset{'}{.}6$ on the 1.23 m f/8 Calar Alto telescope) with a fixed polarization sheet analyzer behind a rotating achromatic $\lambda/2$–plate and uses a 22μ pixel-size GEC chip with 576 x 386 elements. The spectral range of the polarimeter is limited by the polarization sheet analyzer and the $\lambda/2$–plate to 400–750 nm. For the given seeing conditions the FWHM of point sources varied between two and three pixel. Fig. 1 shows our map of total intensity, averaged from the 16 single images.

[2] The DSAZ is operated by the Max-Planck-Institut für Astronomie, Heidelberg, jointly with the Spanish National Commission for Astronomy.

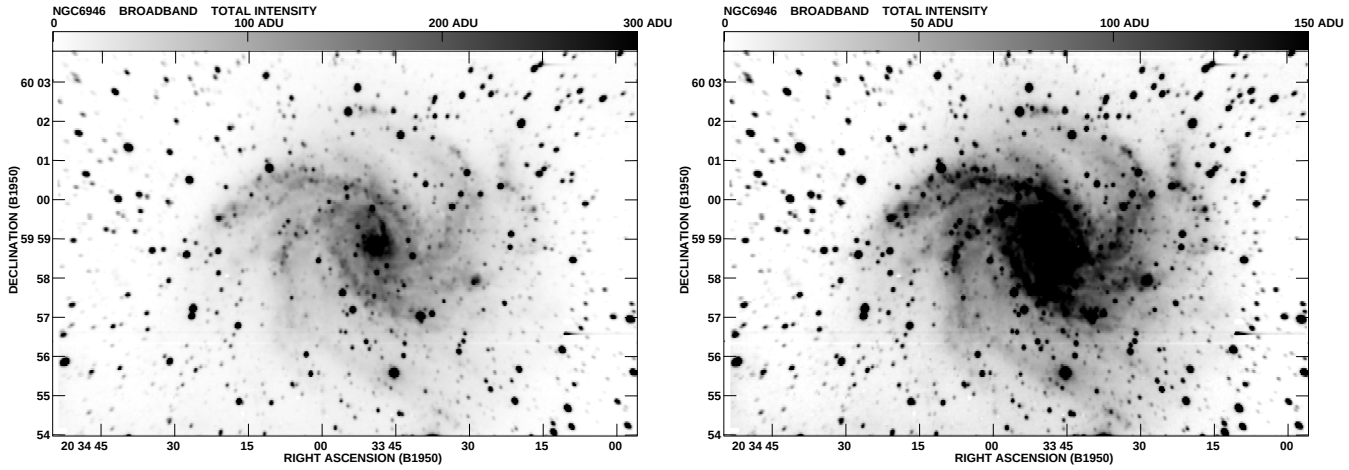

Fig. 1. Total intensity image. The total exposure time was 16x15 min. The field of view is 14.′4 x 9.′6. The greyscale is from 0 to 300 ADU (*left*) and from 0 to 150 ADU (*right*)

3.1. Principle of measurement

The $\lambda/2$–plate is rotated in 16 steps of $22.^\circ5$. Thus, the orientation of incoming polarized light is turned twice per revolution. The normalized ideal signal $S(\Phi_i)$ measured on the detector varies with position Φ_i of the $\lambda/2$–plate as

$$S(\Phi_i) = 1 + P_{\rm x}\cos(4\Phi_i) + P_{\rm y}\sin(4\Phi_i)\,, \qquad (1)$$

with the normalized Stokes parameters $P_{\rm x} = P\cos(2\Theta)$ and $P_{\rm y} = P\sin(2\Theta)$. P and Θ denote the degree of polarization and the polarization angle, respectively. The Stokes parameters are $I_{\rm x} \equiv I\,P_{\rm x}$, $I_{\rm y} \equiv I\,P_{\rm y}$, and the polarized intensity is $I_{\rm P} \equiv I\,P$ with I being the total intensity. Using discrete Fourier analysis, the polarization follows from the $4\Phi_i$ Fourier components,

$$P_{\rm x} = \frac{1}{8}\sum_{i=1}^{16} S(\Phi_i)\cos(4\Phi_i)\,, \quad P_{\rm y} = \frac{1}{8}\sum_{i=1}^{16} S(\Phi_i)\,\sin(4\Phi_i)\,,$$

$$P = \sqrt{P_{\rm x}^2 + P_{\rm y}^2}\,, \quad \Theta = \frac{1}{2}\arctan\frac{P_{\rm y}}{P_{\rm x}} + \frac{m\pi}{2}\,, \qquad (2)$$

where m controls the orientation of the polarization vector with respect to the $P_{\rm x}$–$P_{\rm y}$ space. The absolute polarization angle was calibrated with several polarized standard stars (see P1).

Eq. (1) holds for an ideal signal. Practically, other Fourier frequencies add to the $4\Phi_{\rm i}$ signal, and the real modulation is a superposition of 8 Fourier components caused by various effects (see P1). As a measure for the error in the degree of polarization ΔP, we take the mean of the amplitudes $P_{\rm x}^n$, $P_{\rm y}^n$ of additional Fourier components of other than of fourth order,

$$\Delta P = \frac{1}{5}\left(\sqrt{(P_{\rm x}^3)^2 + (P_{\rm y}^3)^2} + \sum_{n=5}^{8}\sqrt{(P_{\rm x}^n)^2 + (P_{\rm y}^n)^2}\right). \qquad (3)$$

The error in the polarization angle $\Delta\Theta$ can then be approximated by $\Delta\Theta \simeq \frac{1}{2}\arctan(\Delta P/P)$.

3.2. Data reduction

Following the standard CCD data reduction for each frame separately (subtraction of bias, dark current and sky background; flatfielding), additional steps are required in order to combine and compare all 16 frames together. These steps are: • convolution to the same (worst) seeing, • linear offset reduction (rebinning), • (relative) flux calibration. Finally, • Fourier analysis provides the polarization images, i.e. P, ΔP, Θ for each pixel. Note that most of the large-scale foreground polarization is automatically removed in our data reduction with by calibrating the flux with foreground stars. Similarly, a possible sky background polarization is removed by the background subtraction (see P1 and next section).

3.3. Sky background polarization and foreground stars

NGC 6946 is a quite extended object on sky which fills most of our field of view (Fig. 1), different to e.g. M 82 shown in the Appendix. The HI distribution even extends to a radius of 10′ (Tacconi & Young 1986; Kamphuis & Sancisi 1993). Due to the large size of the galaxy, the determination of the background level is difficult, because only relatively small areas of the CCD image are free of emission from the galaxy.

The degree of polarization of the sky background is relatively high, but in most regions statistically distributed with different vector orientations and large errors.

As a test, we chose different values of the background sky intensity. Consequently, the background polarization vectors change their orientation slightly, whereas the polarization vectors in the galaxy are not affected. With the subtraction of a constant sky background intensity in each of the 16 frames, the vectors in the background regions showed some systematic orientation indicating that the subtraction of a *constant* sky background is not fully satisfying. We therefore calculated the background intensity as a linear 2D function based on the intensity distribution in the regions most distant from the galaxy.

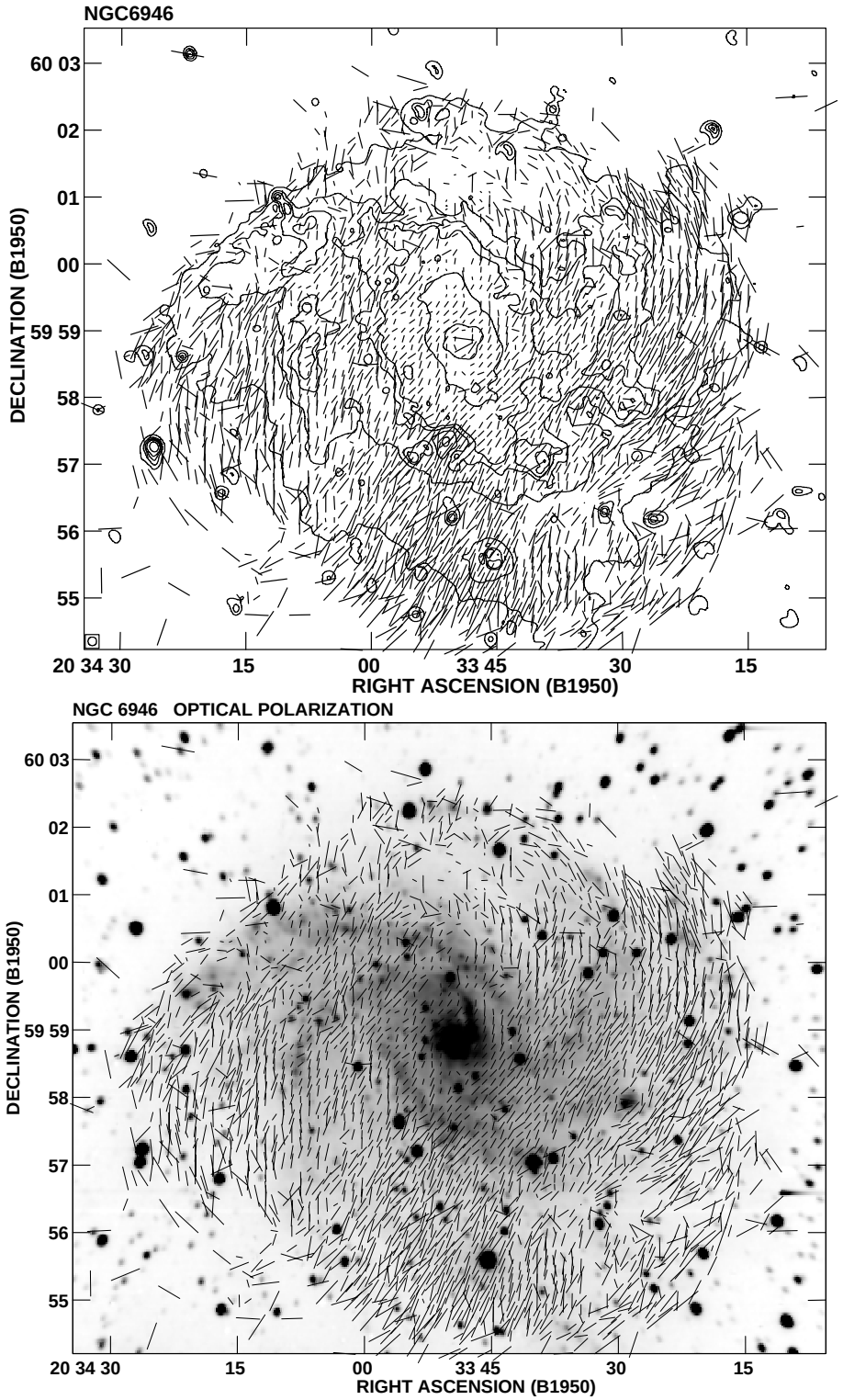

Fig. 2. Linear optical polarization over the full frame observed for NGC 6946. We show only vectors for $0.1\% \leq P \leq 5\%$, $\Delta P \leq 0.3P$, where P is indicated by the length of the vectors (5% degree of polarization corresponds to $15''$ vector length). *above* Polarization (E-)vectors superimposed by contours of total intensity smoothed by a 5x5 median filter. *below* Polarization (E-)vectors superimposed by the mean total intensity image.

This procedure led to a good background estimate, resulting in an almost vanishing mean background polarization.

The systematic error in the background intensity, here defined as the variance of the background intensity over the whole frame, is about ± 0.7 ADU over the whole frame, and ± 0.4 ADU over the region of the galaxy. From the definition of the polarization, $P \equiv (I_{\max} - I_{\min})/2I$, we estimate the error in polarization $\Delta P = P \simeq 0.2/I\,[\mathrm{ADU}]$, corresponding to an artificial polarization of $P \simeq 0.2\%$ for an intensity $I = 50$ ADU and $P \simeq 1\%$ for an intensity $I = 10$ ADU.

Since this error is systematic (as it is due to the uncertainty in the background determination), and not statistical (like photon noise), it cannot be diminished by calculating mean Stokes parameters over several pixels. Thus, some of the high degrees of

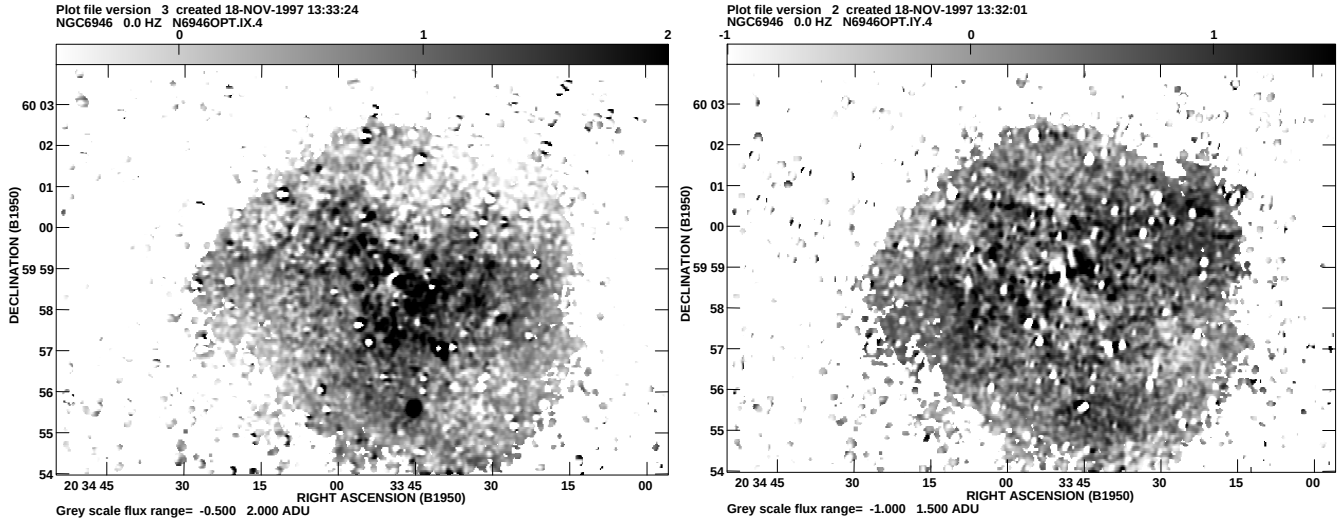

Fig. 3. Image representation of the Stokes parameters $I_{\rm x}$ (*left*) and $I_{\rm y}$ (*right*), greyscale from -1.0 to 1.5 ADU. A running mean filter with a size of 5 pixel radius was applied to the original data. Negative values correspond to polarization angles between 45° and 135° ($I_{\rm x}$), or between 90° and 180° ($I_{\rm y}$) (s. Eq. 1).

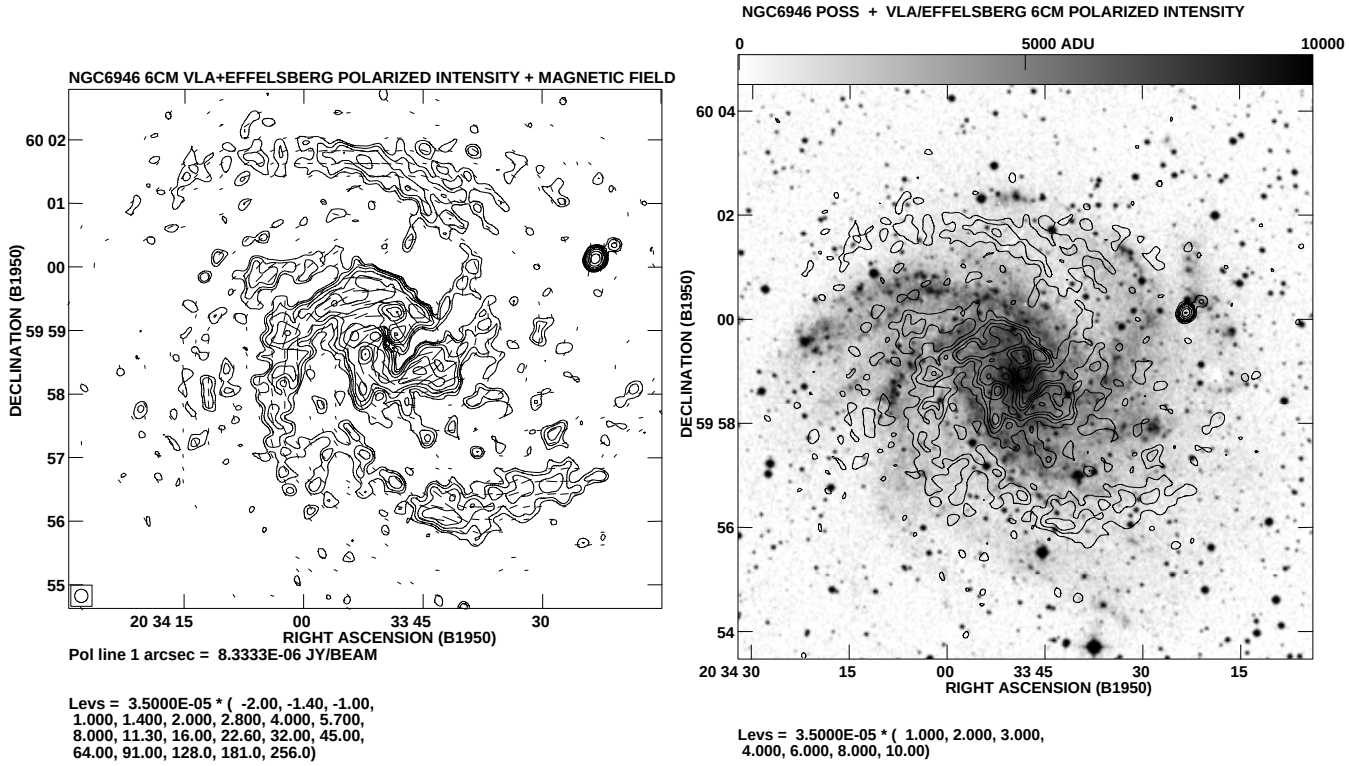

Fig. 4. Comparison with radio data. Polarized radio intensity (6cm) and magnetic field vectors (*left*). Polarized radio intensity (6cm) and optical image from the POSS archive (*right*).

polarization in the low intensity regions may be affected by the background reduction. We therefore have to exclude regions of very low intensity from our consideration, and show only vectors with $P \leq 5\%$ avoiding all vectors with arbitrarily high degrees of polarization outside of the galaxy. Vectors with high errors ΔP, but small P are removed by defining the error limit $\Delta P/P$. Note that bad CCD rows were not removed, since the involved polarization error is very large. These polarization vectors are not considered in the figures.

In the final images (Figs. 1-3,5) the foreground stars show no polarization (except in their wings with steep intensity gradients) indicating a proper flux calibration. As we mentioned above, the foreground polarization between the flux calibration stars and the observer is removed automatically.

From the polarization maps of Behr (1959) and Mathewson & Ford (1970) at the position of NGC 6946 we derive a possible, large-scale Galactic foreground polarization with a polarization degree of $\leq 0.5\%$ and a polarization angle of $135°$. This is much below the degrees of polarization in the outer part of the galaxy and thus cannot affect our data.

3.4. Comparison data

We would like to increase the reader's confidence in our results by showing comparison data of the edge-on star-burst galaxy M 82 from the same observation run and identical data reduction. We find an almost circular polarization pattern (Fig. A1) as already known from the literature (Bingham et al. 1976; Scarrott et al. 1991b). Deviations may arise from the lack of sensitivity and difference in spectral range (Scarrott et al. observed in Hα). Note that previously published results (Fendt et al. 1996) were from the same observational run and did undergo the same procedure of data reduction. We are therefore convinced that the optical polarization patterns of NGC 6946 presented here are real.

4. Results

The optical polarization of NGC 6946 is shown in Figs. 2, 3 and 5. The maps display the orientations of the polarization vectors superimposed on isocontours of the mean total intensity I (Fig. 1), and the Stokes parameters $I_{\rm x}$, $I_{\rm y}$ (Fig. 3). The polarization signal in Figs. 2 and 3 is smoothed with a 5x5 running median filter in order to increase the signal-to-noise ratio of the polarized intensity. Note that there are about 750 foreground stars visible in the field of view.

We plot all polarization (E-)vectors within a chosen limit, $P_{\rm min} \lesssim P \lesssim P_{\rm max}$, and below a certain upper limit for their error $\Delta P/P$. With $|\Delta P| < 0.3P$ (as in Fig. 2) the error in the polarization angle is about $|\Delta\Theta| < 9°$. With a more stringent limit many vectors disappear, but the main features remain visible.

In general the degree of polarization is between 1% – 2% in the inner parts and 3% – 5% in the outer parts of the galaxy (Fig. 2). Along the outermost intensity contour, below $\simeq$ 10 ADU (linear instrumental unit, 1 ADU $\equiv$ 16 electrons) above the background, the polarization reaches sometimes 10%. The latter data should be taken with care since they strongly depend on the background subtraction (see Sect. 3.3). As a consequence, we did not plot any vectors with $P \geq 5\%$ in our figures. The distribution of the *degree* of polarization gives indication that the north-western part of the galaxy is closer to the observer (see Appendix).

The images of the Stokes parameters $I_{\rm x}$ and $I_{\rm y}$ (Fig. 3) prove that the light from NGC 6946 is linearly polarized. Both images show a butterfly-like pattern, with a rotational shift of about $45°$ (for a further interpretation note that the instrumental angular offset of $-40°$ was not applied in this representation). The butterfly pattern, which is a general, well-known feature also for radio polarization observations, is a signature for axisymmetric (circular, elliptical, spiral) distributions of polarization vectors. A constant foreground polarization would lead to constant Stokes parameters.

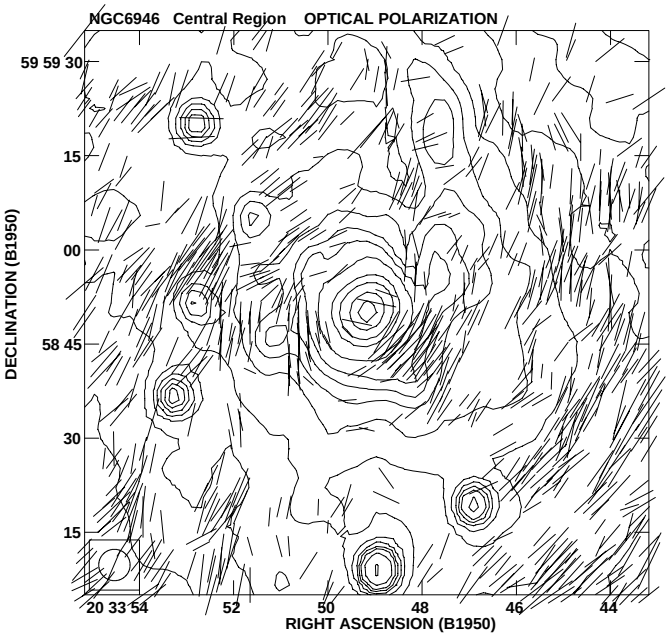

Fig. 5. Linear optical polarization in the center of NGC 6946. Polarization (E-)vectors superimposed by total intensity contours. Enlarged subset, scale 100 pixel $\equiv 2\farcm5$. No averaging for the polarization degree was done. $0.1\% \leq P \leq 5\%$, $\Delta P \leq 0.5P$. The polarization degree is indicated by the length of the vectors, (5% degree of polarization corresponds to $15''$vector length).

The observed degrees of polarization of 1% – 3% are in the range expected by the DGM as well as AS. Scattering models give a maximum polarization for face-on galaxies of 1% – 2% (Bianchi et al. 1996, Wood & Jones 1997, Wood 1997). We therefore have to weigh up between the two competing processes DGM and AS. We know from radio polarization observations (Beck & Hoernes 1996) that the regular field in NGC 6946 is strong and of spiral shape. The scattering models (Bianchi et al. 1996, Wood & Jones 1997, Wood 1997), on the other hand, are rather general and do not take into account the spiral structure.

5. Discussion

5.1. The galaxy center

The polarization pattern of the central region is shown in Fig. 5. To obtain highest spatial resolution, we did not average over several pixels. Therefore the error ΔP is higher, and the threshold $\Delta P/P$ has to be increased to 0.5 in order to plot reliable vectors only.

In the central region we find a roughly circular pattern. This demonstrates that foreground polarization towards the center was subtracted successfully. This circular polarization pattern may easily explained by AS of the bright nucleus. The intensity contrast between the central pixel and a distance of 10 pixels is of the order of 10. It is known from molecular and infrared data

that this central region is the location of massive star formation (Roy & Belley 1993). The therefore required interstellar matter of high density would perform ideal scattering sources, but may also lead to multiple scattering.

The polarization in the central northern arm emanating from the nucleus is perpendicular to this arm. This pattern deviates from the neighboring region. In the case of AS and optically thin conditions within the arm, the polarization pattern would expected to be aligned with the orientation of the arm, since the light distribution gradient is perpendicular to the arm. AS of light from the galaxy center would result in a polarization pattern perpendicular to the observed one. On the other hand, it is known from radio observations that the magnetic field in this region is aligned with the arm. If we adopt the DGM as the cause of polarization, the deduced magnetic field would be in contradiction to the radio observations.

A particularly interesting feature is the apparent *lack* of polarized intensity south of the nucleus of the galaxy, where the polarization vanishes within an area of several arcseconds extent. Here, the total intensity image shows no deviation from a circular/elliptical shape. This region of unpolarized optical emission coincides with a molecular bar found in Hα and CO data (Ishizuki et al. 1990; Roy & Belley 1993; Regan & Vogel 1995). The CO molecular bar emanates from the center of the galaxy at the same orientation as the region of low optical polarization (i.e. P.A. $165°$). Why is this molecular bar less optically polarized?

The first possibility is that the light is intrinsically unpolarized. Anisotropic scattering in a *homogeneous* distribution of light and dust leads to vanishing polarization. Such a homogeneous distribution is not very likely, since the bright central light source dominates the light distribution.

The second possibility is that two polarizing processes cancel. AS of light from the galactic center generates a circular pattern, i.e. a P.A. of about $45° - 90°$ in this region. If there is an additional polarizing mechanism producing a polarization with an angle of $135° - 180°$, the polarization due to AS would be destroyed. If we assume polarization due to the DGM in a regular magnetic field along the bar (as indicated by the radio polarization data), this pattern cancels with the AS polarization south of the center.

A third possibility is that we see mainly stars above the dust disk of NGC 6946 which are much less polarized, while light light from deeper layers is fully absorbed.

5.2. The spiral arms

In general, the polarization vectors follow a spiral pattern in the eastern and western parts of the galaxy (Fig. 2). The spiral pattern is seen along the arms as well as in the interarm regions between the western and eastern spiral arms (with larger errors due to the lower intensity). In particular, the spiral polarization pattern is most regular in the outer arm in the west and northwest, although the optical spiral structure appears disturbed in these regions.

In comparison with the map of the fractional polarization, the polarized intensities (Fig. 3) has a lumpy structure. This is partly due to the large number of foreground stars, which were not totally removed. However, there are clearly elongated structures visible. These structures follow in general a spiral pattern and are aligned with the optical arms.

The origin of the optical polarization could be by AS or DGM. To generate a spiral pattern by AS, simple geometric considerations suggest that a systematic spatial shift between light sources and scattering centers may be required. However, NGC 6946 does not possess narrow dust lanes at the edges of spiral arms. Light, gas and dust appear well mixed in all spiral arms.

We thus propose that the optical polarization spiral pattern could be due to DGM and is complement to the radio data concerning the overall magnetic field structure. The optical data also show the small-scale components of the magnetic field, not resolved by the radio observations.

There are several extended regions where the optical polarization is weak: the massive spiral arm in the northeast, the spiral arms north and south of the center, the northern interarm region and an interarm region in the southwest. If in some region no optical polarization is detected, this could just be due to a low intensity corresponding to a large error in polarization. However, this is not the case for the spiral arm and interarm regions mentioned above.

Some regions of unpolarized optical emission tend to coincide with spiral-arm regions where Hα emission is strong (Ehle & Beck 1993).

The increasing star formation might destroy part of the dust grains and mix up the remaining population such that no single-scattering process remains for significantly large areas. Thus, the polarization by AS decreases. In the DGM picture, the observed lack of optical polarization might be explained by magnetic field tangling due to star-formation activity. The same effect also decreases the polarized intensities in radio emission (Beck & Hoernes 1996). The radio data have a lower resolution ($\simeq 330$ pc at the assumed distance to NGC 6946). With averaging over 3x3 pixels we achieve $\simeq 120$ pc, and the degree of optical polarization in the NE arm still remains very low. Without averaging, the errors become too large so that no statements about the field tangling on a scale of 40 pc are possible.

In the northern and southern interarm regions, located between the most prominent optical spiral arms, the degree of optical polarization is below 0.5%, in sharp contrast to the "magnetic arms" observed in radio polarization with up to 30% polarization (Beck & Hoernes 1996; see Fig. 4). This can also be understood in terms of the DGM. In spite of a strong and regular magnetic field in the interarm region, the lack of dust cannot generate significant optical polarization.

The optical polarization pattern in NGC 6946 joins perfectly to the radio polarization pattern (Fig. 4) observed by Beck & Hoernes (1996), except for the southern region (see next section) and north of the nucleus. Field tangling by star-formation activity affects the degree of polarization of both the optical and radio emission. The agreement between the two spectral domains

provides a strong argument that the *same magnetic field* is responsible for both the DGM and for the polarized synchrotron emission.

5.3. Optical polarization in the southern and southwestern regions

In the southern and southwestern regions the polarization pattern is neither circular nor spiral, but shows two different signatures (see Fig. 2):

(1) A well-aligned polarization structure in the south of NGC 6946 with almost constant polarization angles of about $155°$. This region extends from close to the galaxy center over a large scale of about $3'$.

(2) A region in the southwest (SW) of the galaxy of chaotic polarization angle distribution, with radial as well as tangential orientations and also regions with vanishing polarization.

Our tests with different levels of background subtraction have convinced us that these features are real. Feature (2) can be understood by a less regular distribution of magnetic field or a lack of an appropriate distribution of stars or dust (see Sect. 5.3.2), but feature (1) is obviously anomalous.

5.3.1. Polarization by a cloud in the Galactic foreground?

The observed polarization features can hardly be explained by scattering models of a simple spiral disk. Especially feature (1), extending across the spiral arms without any change of polarization angle, would require a similar, constant large-scale distribution of scattering sources (light and gas/dust), which is in conflict with the total intensity image.

The other possibility, DGM, also runs into difficulties, since the required large-scale field alignment was not recognized by radio observations. If we compare the orientation of the radio B-vectors (Ehle & Beck 1993, Beck & Hoernes 1996) to the optical polarization vectors south of the center, we find that they are almost *perpendicular* to each other. (We note that similar deviations were also found in M 51, see Beck et al. 1987.) The radio polarization data of NGC 6946 do not indicate a deviation from a spiral pattern in the south, though the polarized intensities are somewhat low there. Faraday rotation and radio depolarization are exceptionally strong in the SW quadrant which may indicate non-spiral magnetic fields along the line of sight, i.e. emerging from the galaxy's plane (Beck 1991). However, such a field should not produce optical polarization because DGM is sensitive only to the magnetic field components in the plane of the sky.

If feature (1) is intrinsic, it should be affected by the spiral structure. This is not the case. Thus we have to consider an origin external to NGC 6946 for the large-scale alignment of polarization in the southern region. A comparison with the total intensity image shows that the anomalous polarization region extends across the arm - interarm region towards the eastern quadrant. This might indicate that the observed pattern is caused by *locally enhanced (Galactic) foreground polarization* due to a magnetized molecular/dust filament between the foreground stars and NGC 6946.

We emphasize that NGC 6946 is located close to the Galactic plane and might suffer from considerable extinction. The polarization angle is similar to the foreground polarization in our Galaxy deduced from the polarization maps of Behr (1959) and Mathewson & Ford (1970). However, since the general degree of foreground polarization is rather low ($\leq 0.5\%$), the polarizing medium must enhance the effectiveness of the DGM, maybe by an increase of the strength of the general Galactic interstellar magnetic field by compression.

The size of the anomalous region is about $3'$ in diameter. This would correspond to a cloud size of $\simeq 1\,\mathrm{pc}\,(d/3')(D/1\,\mathrm{kpc})$, where D is the distance of the cloud from the observer. This is a typical size for small molecular clouds. From observation of interstellar polarization in the Galaxy we know the correlation between extinction A_v and optical polarization, $P \simeq 0.015 A_\mathrm{v}$. Thus, a foreground polarization of 2-3% would correspond to an extinction of $A_\mathrm{v} \simeq 2$, which should clearly be detected. No signature for such a cloud is visible in any tracer of interstellar gas.

We conclude that normal galactic foreground polarization cannot account for the polarization pattern in the southern part of NGC 6946. A kind of "magnetic cloud" would be necessary, i.e. a region of enhanced magnetic field strength or enhanced alignment of the field without an increase of mass density. Only with such a hypothetical object an increased local foreground polarization without optical absorption can be explained.

In summary, the cause of the polarization pattern in the southern part of NGC6946 remains unclear. We believe that the observed polarization is real, but the astrophysical interpretation is still missing.

5.3.2. Depolarization in the southwestern region

The low degrees of optical polarization in the southwest region may be interpreted in various ways.

First, the general distribution of stars and dust could be inappropriate for any kind of polarization mechanism. An isotropic mixing would prevent the AS from causing polarization and a lack of reasonably extended dust clouds would yield the DGM invisible.

Second, the general structure could be more chaotic than elsewhere. The optical spiral structure is much less developed than in the other parts of the galaxy. Regular magnetic fields are only occurring in the southern "magnetic arm" (Beck & Hoernes 1996) which is probably void of dust and thus cannot serve for the DGM.

The FIR continuum observations show indication for two dust components in the galaxy. While the cool dust (20K) component, tracing the general interstellar medium, peaks in the northeastern arm region, the warm dust (30K) component, tracing regions of star formation, is dominant in the southwestern region of the "flocculent" arm region (Engargiola & Harper 1992). The authors suggest a more "stochastic" star formation

in the SW compared to a recent star formation burst in the NE arm.

The SW part of the galaxy shows irregularities also in other frequency bands. Tacconi & Young (1990) found differences between the NE and SW region in the correlation of H_2 surface density enhancement with that of Hα flux and the Hα/H_2 ratio. They correlated these ratios with the massive star formation efficiency (Hα/H_2) and the recent to the past star-formation rate (Hα/B–band). The ratios Hα/H_2 and Hα/B–band are smaller in the SW region at a radius of $3'$. (However, at a smaller radius of $2\farcm25$, where an optical arm is visible, these ratios are of the same order as in northern optical arms.)

Kamphuis & Sancisi (1993) reported large-scale differences in the high-velocity gas distribution between the two sides of the galaxy. There is more high-velocity gas in the SW region, which indicates enhanced vertical motions of the HI gas. Most of the high velocity features are detected where the HI emission is weak. The mean velocity dispersion decreases from $13\,\mathrm{km\,s^{-1}}$ in the optical turbulent disk to $6\,\mathrm{km\,s^{-1}}$ in the outer parts, where the HI is fainter and follows a regular spiral pattern.

DGM would be also invisible in the presence of vertical magnetic fields. From Faraday rotation and depolarization data in the radio regime, Beck (1991) found evidence for such vertical fields in the SW region. His suggestion of a galactic "coronal hole" received tentative support by *ROSAT* data, where Schlegel (1994) found indication for a lack of X-ray emission in the SW region of NGC 6946.

Combining the results from Beck (1991), Tacconi & Young (1990) and Kamphuis & Sancisi (1993), there are many hints of a lack of organized star formation in the SW region and possibly vertical field components, all of which may lead to a low degree of optical polarization - for both possible mechanisms.

Alternatively, the lack of polarized emission in the SW region might probably be explained by mixing of light polarized at angles perpendicular to each other. If we suppose that the spiral polarization pattern of the western arm intrinsically continues towards the south, this pattern would become perpendicular to that of the southern anomalous region within the SW region. Since both pattern have a similar degree of polarization, they cancel.

We favor the latter explanation, where the deduced magnetic fields are simply of spiral shape, in agreement with the radio data, and no vertical field is necessary. The radial polarization pattern in the south is due to some unknown foreground effect (see Sect. 5.3.1).

6. Conclusions

We presented linear optical polarization maps of the face-on spiral galaxy NGC 6946. The main polarization structures are (1) a roughly spiral pattern along the optical arms, and (2) a radial pattern in the region south of the center. There are also regions where (3) no polarization could be detected. A circular polarization pattern (4) in the center of the galaxy demonstrates proper subtraction of the mean foreground polarization. The inner northern arm close to the center is polarized perpendicular to the arm orientation, which cannot be explained by anisotropic scattering.

The spiral pattern (1) is seen with almost no contrast along the arms as well as in the interarm region of the western and eastern arms. Since we know from radio observations that a large-scale spiral magnetic field is present in the galaxy, the spiral optical polarization feature can be interpreted as due to the Davis-Greenstein mechanism (DGM). In contrast to the radio data, the optical polarization in the northern and southern outer interarm regions is generally low. However, since any scattering mechanism relies on selective extinction of *dust* grains and there is little interstellar dust in the interarm regions, it is understandable that no polarization could be detected in spite of strong regular magnetic fields.

Some of the brightest regions within the spiral arms are unpolarized ($P < 0.5\%$). These regions coincide with strong Hα emission. We propose that strong star-formation activity tangles the large-scale magnetic field and thus reduces the large-scale alignment of dust grains as an essential requirement for the operation of the DGM. This interpretation is in agreement with the radio observations, where a similar effect is observed. Anisotropic scattering would also suffer from the more chaotic conditions in regions of increased star-formation activity.

The polarization pattern with a radial orientation (2) in the southern part of the galaxy remains an open question. Anisotropic scattering seems to be ruled out by geometrical arguments. An operating DGM is similarly unlikely since the magnetic fields observed in radio polarization follow a spiral, not a radial pattern. The possibility that the optical polarization detects a field different from the radio polarization (i.e. the field in the thin dust disk and not a field in the thick radio disk), seems not very plausible. We therefore propose that this polarization pattern might be caused by enhanced foreground polarization, due to a locally compressed interstellar magnetic field. The size of the region corresponds to $\simeq 1$ pc at Galactic distances.

From the fractional polarization along the minor axis in the central region of the galaxy we find weak indication that the northwestern side is closer to the observer, in agreement with radial velocity measurements and the common belief that spiral arms are trailing.

Finally we emphasize that our interpretation of the optical polarization data should be taken with the natural care, since realistic scattering models of spiral galaxies are not yet available and the theory of the Davis-Greenstein mechanism is not yet fully understood (although it seems to explain many features in the Galaxy). We hearty encourage model calculations of anisotropic scattering in spiral galaxies, taking into account more realistic distribution of light and dust, i.e. the spiral signature of these galaxies.

Acknowledgements. The Max-Planck-Gesellschaft is acknowledged for financial support of the project, and the staff of the DSAZ for help during the observations. We are grateful to R. Wielebinski for his continuous support for this project. C.F. appreciated the visitorship at the Max-Planck-Institut für Radioastronomie in spring 1997.

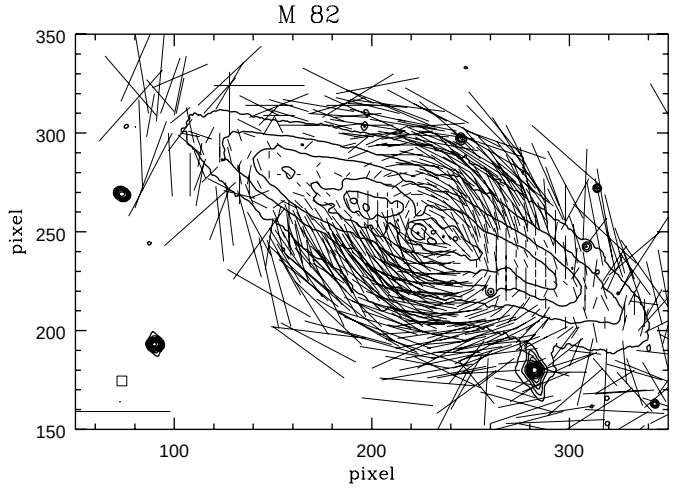

Fig. A1. Comparison example. Linear optical polarization of M 82. Polarization (E-)vectors superimposed by total intensity contours. $0.1\% \leq P \leq 10\%$, $\Delta P \leq 0.3P$. The polarization degree is indicated by the length of the vectors. Contour levels = 16, 32, 64, 128, 256, 512, 1024 ADU. The elongated shape of the stars are due to a IR blocking filter (exchanged later). Enlarged subset of the original frame. The polarization degree is averaged over 5 x 5 pixels; 10% correspond to 50 pixels

Appendix A: comparison data of M 82

Here we present an optical polarization map of the well known galaxy M 82 (Fig. A1). The galaxy was observed during the same observation run with the same equipment and we applied the same data reduction software as in the case of NGC 6946. The resulting large-scale circular polarization pattern is well known from the literature (Bingham et al. 1976; Neininger et al. 1990; Scarrott et al. 1991b).

Appendix B: orientation of NGC 6946 towards the plane of sky

In the following we discuss whether the orientation of NGC 6946 with respect to the sky plane could be determined from optical polarization. As already mentioned by King (1986) and P1 for NGC 7331, interstellar dust is highly forward-scattering. Thus, in a tilted dust disk illuminated by a central light source, the average degree of polarization should be larger on the nearer side of the disk since the scattering angle is larger (and vice versa for the other side).

This was recently confirmed by Monte-Carlo Mie scattering calculations (Bianchi et al. 1996; Bianchi, priv. comm.). In the case of a 20° inclined galaxy (similar to NGC 6946) with a bulge luminosity half of the total luminosity, the authors calculate a polarization pattern such that the degree of polarization along the "minor" axis differs by a factor of two between the near and the far sides.

The latter arguments are valid only if interstellar *dust* is the main scattering source. For small particles, molecular and atomic gas, AS should be considered in the Rayleigh limit. In this case, however, the scattering probability is a symmetric function with its maximum at a 90° scattering angle. In the case of Rayleigh scattering the front/near side of the galaxy cannot be determined.

From our polarization maps we find that in the case of NGC 6946 the degree of polarization along the minor axis of the central region is in average slightly larger in the northwest. We only consider the central region, since we suppose that this is the most smooth region in the galaxy. We find a median value from 2500 pixels of $P = 1.8\%$ in the northwest, and $P = 1.5\%$ in the southeast. If we assume that the optical polarization of NGC 6946 partly arises from scattering in the Mie limit, we conclude that the northwestern side is closer to us, in agreement with radial velocity observations (Tacconi & Young 1986). This confirms the common belief that optical spiral arms are trailing.

References

Beck R., 1991, A&A 251, 15
Beck R., Hoernes P., 1996, Nature 379, 47
Beck R., Klein U., Wielebinski R., 1987, A&A 186, 95
Beck R., Brandenburg A., Moss D., Shukurov A., Sokoloff D., 1996, ARA&A 34, 155
Behr A., 1959, Veröffentlichungen der Universitätssternwarte Göttingen 126, 185
Bianchi S., Ferrara A., Giovanardi C., 1996, ApJ 465, 127
Bingham R.G., McMullan D., Pallister W.S. et al., 1976, Nature 259, 463
Carignan C., Charbonneau P., Boulanger F., Viallefond F., 1990, A&A 234, 43
Davis L., Greenstein J.L., 1951, ApJ 114, 206
Ehle M., Beck R., 1993, A&A 273, 45
Elstner D., Meinel R., Beck R., 1992, A&AS 94, 587
Elvius A., 1951, Stockholms Obs. Ann. 17, No. 4
Elvius A., 1956, Stockholms Obs. Ann. 19, No. 1, 3
Engargiola G., Harper D.A., 1992, ApJ 394, 104
Fendt C., Beck R., Lesch H., Neininger N., 1996, A&A 308, 713 (P1)
Frick P., Beck R., Shukurov A., et al., 1998, MNRAS, submitted
Hall J.S., 1949, ApJ 54, 187
Harnett J.I., Beck R., Buczilowski U.R., 1989, A&A 208, 32
Helou G., Malhotra S., Beichman C.A., et al., 1996, A&A 315, L157
Hiltner W.A., 1949, Nature 169, 283
Ishizuki S., Kawabe R., Ishiguro M., et al., 1990, ApJ 355, 436
Kamphuis J., Sancisi R., 1993, A&A 273, L31
King D.J., 1986, MNRAS 220, 485
Klein U., Beck R., Buczilowski U.R., Wielebinski R., 1982, A&A 108, 176
Lu N.Y., Helou G., Tuffs R.J., et al., 1996, A&A 315, L153
Madden S.C., Geis N., Genzel R., et al., 1993, ApJ, 407, 579
Malhotra S., Helou G., van Buren D., et al., 1996, A&A 315, L161
Mathewson D.C., Ford V.L., 1970, Mem. Roy. Astron. Soc. 74, 139
Neininger N., Backes F., Beck R., 1990, in: R. Beck et al. (eds), IAU Symp. 140, Galactic and Intergalactic Magnetic Fields, Kluwer, Dordrecht, p253
Regan M.W., Vogel S.N., ApJ 1995, 452, L21
Rogstad D.H., Shostak G.S., 1973, A&A 22, 111
Roy J.-R., Belley J., 1993, ApJ 406, 60
Scarrott S.M., Ward-Thompson D., Warren-Smith R.F., 1987, MNRAS 224, 299
Scarrott S.M., Rolph C.D., Wolstencroft R.W., Tadhunter C.N., 1991a, MNRAS 249, 16p

Scarrott S.M., Eaton N., Axon D.J., 1991b, MNRAS 252, 12p
Scarrott S.M., Draper P.W., 1996, MNRAS 278, 519
Schlegel E.M., 1994, ApJ 434, 523
Smith J., Harper D.A., Loewenstein R.F., 1984, in: H.A. Thronson, Jr., E.F. Erickson (eds), NASA Conf. Pub. 2353, Airborne Astronomy Symposium Proceedings, p277
Spitzer L., Jr., 1978, Physical Processes in the Interstellar Medium. Wiley, New York
Tacconi L.J., Young J.S., 1986, ApJ 308, 600
Tacconi L.J., Young J.S., 1989, ApJS 71, 455
Tacconi L.J., Young J.S., 1990, ApJ 352, 595
Tully R., 1988, Nearby Galaxies Catalog, Cambridge, Cambridge University Press, p56
Tuffs R.J., Lemke D., Xu C., et al., 1996, A&A 315, L149
Valentijn E.A., van der Werf P.P., de Graauw T., de Jong T., 1996, A&A 315, L145
Wood K., 1997, ApJ 477, L25
Wood K., Jones T.J., 1997, AJ 114, 1405